Note after first publication: **Figures S5a**, **S6a**, and **S9b** have been updated on 13th December 2024 to correct inadvertent errors that occurred during compilation of this document. The corrections do not change or invalidate any of the conclusions reported in the original publication on 8th December 2021.

Supporting Information

Truncation Reaction Regulates Out-to-In Growth Mechanism to Decrypt the Formation of Brucite-like Dysprosium Cluster

Yun-Lan Li,[a,+] Hai-Ling Wang,[a,+] Zhong-Hong Zhu,[a,c,*] Juan Li,[a] Hua-Hong Zou,[a,*] Jin-Mei Peng,[a] and Fu-Pei Liang[a,b,*]

[a]School of Chemistry and Pharmaceutical Sciences, State Key Laboratory for Chemistry and Molecular Engineering of Medicinal Resources, Guangxi Normal University, Guilin 541004, P. R. China

[b]Guangxi Key Laboratory of Electrochemical and Magnetochemical Functional Materials, College of Chemistry and Bioengineering, Guilin University of Technology, Guilin 541004, P. R. China

[c]State Key Laboratory of Luminescent Materials and Devices, School of Materials Science and Engineering, South China University of Technology, 510640 Guangzhou, P. R. China

*E-mail (Corresponding author): 18317725515@163.com (Z.-H. Zhu), gxnuchem@foxmail.com (H.-H. Zou), fliangoffice@yahoo.com (F.-P. Liang).

Table of Contents:

Experimental Section

Materials and Measurements.

All reagents were obtained from commercial sources and used without further purification. Elemental analyses for C, N and H were performed on a vario MICRO cube. Infrared spectra were recorded by transmission through KBr pellets containing *ca.* 0.5% of the complexes using a PE Spectrum FT-IR spectrometer (400–4,000 cm^{-1}; Figure S4). Thermogravimetric analyses (TGA) were conducted in a flow of nitrogen at a heating rate of 5 °C/min using a NETZSCH TG 209 F3 (Figure S5). Powder X-ray diffraction (PXRD) spectra were recorded on either a D8 Advance (Bruker) diffractometer at 293 K (Mo-Kα). The samples were prepared by crushing crystals and the powder placed on a grooved aluminum plate. Diffraction patterns were recorded from 5º to 55º at a rate of 5º min^{-1} (Figure S6). Measurements of magnetic susceptibility were carried out within the temperature range of 2–300 K using a Quantum Design MPMS SQUID magnetometer equipped with a 5 T magnet. The diamagnetic corrections for these complexes were estimated using Pascal's constants, and magnetic data were corrected for diamagnetic contributions of the sample holder. Alternating current susceptibility measurements were performed from powdered samples to determine the in-phase and out-of-phase components of the magnetic susceptibility. The data were collected by increasing the temperature from 2 K to 15 K within frequencies ranging from 10 to 1,000 Hz. In the samples where free movement of crystallites was prevented, silicone grease was employed for embedding.

Single-crystal X-ray crystallography.

The diffraction data of complex **1**–**3** were obtained by Bruker Apex-II CCD diffractometer (Cu-Kα radiation, λ = 1.54184 A); XtaLAB Synergy, Dualflex, Hyix diffractometer (Mo-Kα radiation, λ = 0.71073 A); Data were collected using the ω scanning mode of XtaLAB Synergy, Dualflex, Hyix diffractometer (Cu-Kα radiation, λ = 1.54184 A), respectively. The structures were solved by direct methods, followed by difference Fourier syntheses, and then refined by full-matrix least-squares techniques on F^2 using *SHELXL*[1]. All other non-hydrogen atoms were refined with anisotropic thermal parameters. Hydrogen atoms were placed at calculated positions and isotropically refined using a riding model. The CCDC reference numbers are 2120830, 2091294 and 2091295 for **1**–**3**.

The synthesis method.

Synthesis of 4-diethylamino salicylaldehyde-2,2-bipyridyl-6,6-dimethyhydrazones (H_4L^1) [2]:

2,2-bipyridyl-6,6-dimethyhydrazide (4 mmol, 1.027g) was dissolved in 100 mL of absolute methanol to which 4-diethylaminosalicylaldehyde (24 mmol, 4.732 g) was added and then refluxed at 80 ˚C for 12 h. The resulting yellow solid (2.32 g, 93%) was filter under vacuum, washed methanol followed by drying under reduced pressure.

Synthesis of 1: Add 0.05 mmol (approximately 32.1 mg) ligand H_4L^1, 0.1 mmol $Dy(NO_3)_3·6H_2O$ (approximately 45 mg), 0.1 mmol $DyCl_3·6H_2O$ (approximately 37 mg), 1.5 mL CH_3OH, 0.5 mL CH_3CN and 0.10 mL triethylamine to the Pyrex tube. In the tube, shake and sonicate for 15 min. Place the sealed Pyrex tube in an oven at 80 ˚C, take it out two days later, slowly cool to room temperature, and precipitate yellow lumpy crystals. The yield is about 44% (calculated with the amount of $Dy(NO_3)_3·6H_2O$). Elemental analysis theoretical value ($C_{100}H_{153}Cl_8Dy_{16}N_{30}O_{73}$): C, 20.62%; H, 2.65%; N, 7.22%; experimental value: C, 20.07%; H, 2.10%; N, 6.98%. Infrared spectrum data (IR, KBr pellet, cm^{-1}): 3435(s), 1567(s), 1510(m), 1461(m), 2982(w), 1235(w), 2929(vs), 725(w), 1130(m), 1638(s).

Synthesis of 2: Add 0.05 mmol (approximately 32.1 mg) ligand H_4L^1, 0.2 mmol $DyCl_3·6H_2O$ (approximately 76 mg), 0.1 mmol pivalic acid (approximately 10.2 mg), 1 mL CH_3OH, 1 mL CH_3CN, and 0.10 mL triethylamine to the Pyrex tube. In the tube, shake and sonicate for 15 min. Place the sealed Pyrex tube in an oven at 80 ˚C, take it out two days later, slowly cool to room temperature, and precipitate yellow lumpy crystals. The yield is about 45% (calculated with the amount of $DyCl_3·6H_2O$). Elemental analysis theoretical value ($C_{100}H_{185}Cl_6Dy_6N_{20}O_{41}$): C, 34.27%; H, 5.32%; N, 7.99%. Experimental value: C, 33.63%; H, 5.01%; N, 7.68%. Infrared spectrum data (KBr pellet, cm^{-1}): 3445(s), 2974(w), 2916(vs), 1610(s), 1518(s), 1473(m), 1372(m), 1334(m), 1243(m), 1133(m), 702(m), 617(m).

Synthesis of 3: Add 0.05 mmol (about 32.1 mg) ligand H_4L^1, 0.1 mmol $Dy(NO_3)_3·6H_2O$ (about 45 mg), 0.1 mmol $DyCl_3·6H_2O$ (approximately 38 mg), 0.1 mmol di(pyridin-2-yl)methanone (about, 18.4 mg), 1 mL CH_3OH, 1 mL CH_3CN and 0.10 mL triethylamine to the Pyrex tube. In the tube, shake and sonicate for 15 min. Place the sealed Pyrex tube in an oven at 80 ˚C, take it out two days later, slowly cool to room temperature, and precipitate yellow lumpy crystals. The yield is about 41%

(calculated with the amount of ligand). Elementary analysis theoretical value ($C_{66}H_{113}Cl_2Dy_7N_{20}O_{45}$): C, 25.11%; H, 3.61%; N, 8.87%. Experimental value: C, 24.43%; H, 3.21%; N, 8.16%. IR data (cm^{-1}): 3445(s), 2984(w), 2895(vs), 1586.21(s), 1379(s), 1231(m), 1059(m), 883(m), 709(w).

Table S1. Crystallographic data of the clusters **1**–**3**.

	1	**2**	**3**
Formula	$C_{100}H_{153}Cl_8Dy_{16}N_{30}O_{73}$	$C_{100}H_{185}Cl_6Dy_6N_{20}O_{41}$	$C_{66}H_{113}Cl_2Dy_7N_{20}O_{45}$
Formula weight	5823.06	3504.05	3156.87
T, K	293(2)	100.00(10)	100.00(10)
Crystal system	trigonal	monoclinic	monoclinic
Space group	*R*-3*c*	$P2_1/n$	*C*2/*c*
a, Å	31.8024(5)	15.4667(3)	24.1218(4)
b, Å	31.8024(5)	26.7576(4)	19.51008(19)
c, Å	32.0143(7)	16.1721(4)	22.0893(3)
α, °	90	90	90
β, °	90	113.181(2)	105.4542(10)
γ, °	120	90	90
V, Å^3	28041.1(10)	6152.5(2)	10019.7(2)
Z	12	1	1
D_c, g cm^{-3}	2.226	1.642	1.971
μ, mm^{-1}	6.43	3.80	28.640
F(000)	15233.0	2982.0	5706.0
2θ range for data collection/°	4.668, 60.12	4.1, 61.4	6.0, 154.4
Reflns coll.	40405	53113	37561
Unique reflns	5506	15438	9976
R_{int}	0.0349	0.0364	0.0413
Observed data [$I >$ 2$\sigma(I)$]	4671	12744	11525
N_{ref}, N_{par}	5506, 344	735, 1588	2, 605
R_1[a] ($I > 2\sigma(I)$)	0.0494	0.0392	0.0568
wR_2[b] (all data)	0.1474	0.1233	0.1523
GOF	1.081	1.055	1.016

[a]$R_1 = \Sigma||F_o|-|F_c||/\Sigma|F_o|$, [b]$wR_2 = [\Sigma w(F_o^2-F_c^2)^2/\Sigma w(F_o^2)^2]^{1/2}$

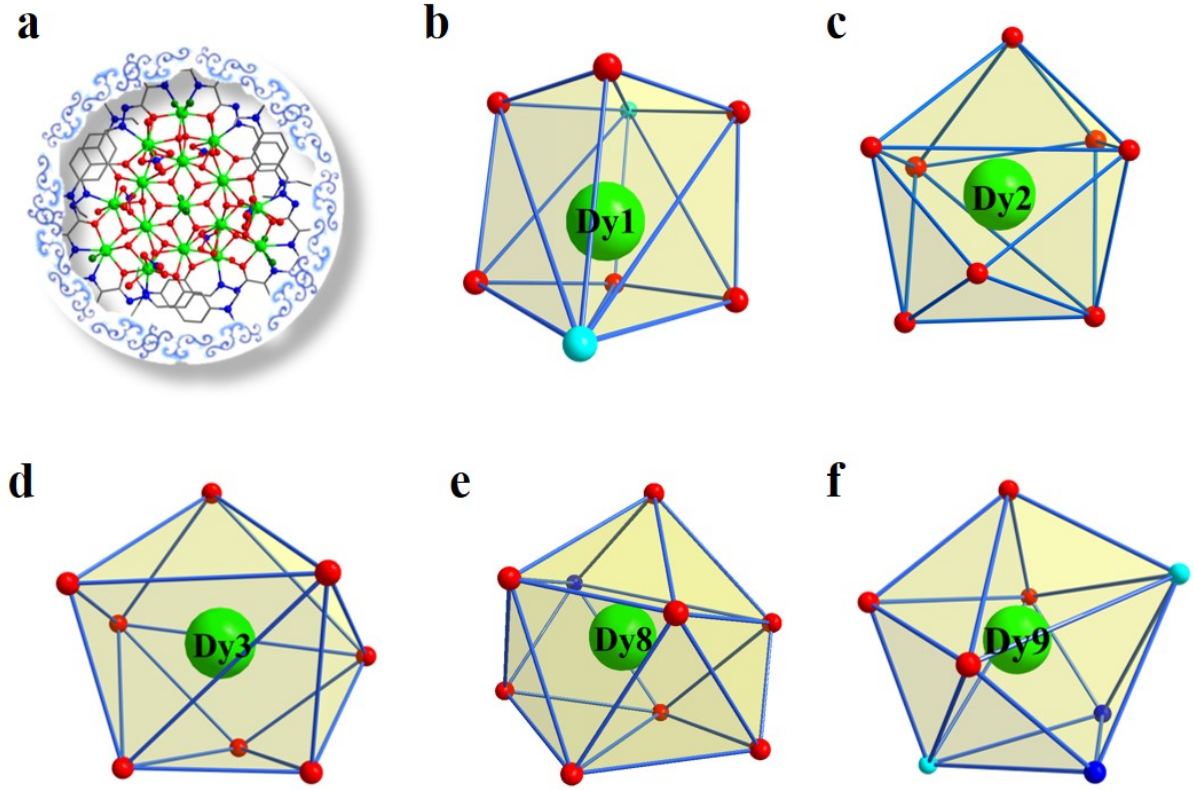

Figure S1. The crystal structure of cluster **1** (a); the coordination environment of metal centers Dy1, Dy2, Dy3, Dy8 and Dy9 in cluster **1** (b–f).

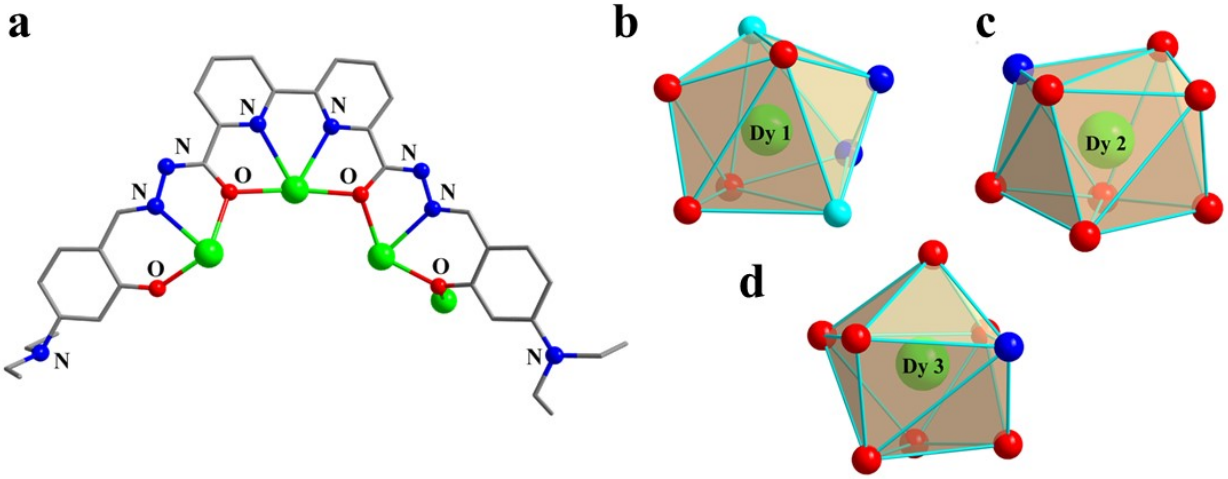

Figure S2. Ligand $(L^1)^{4-}$ coordination mode (a); the coordination environment of metal centers Dy1-Dy3 in cluster **2** (b).

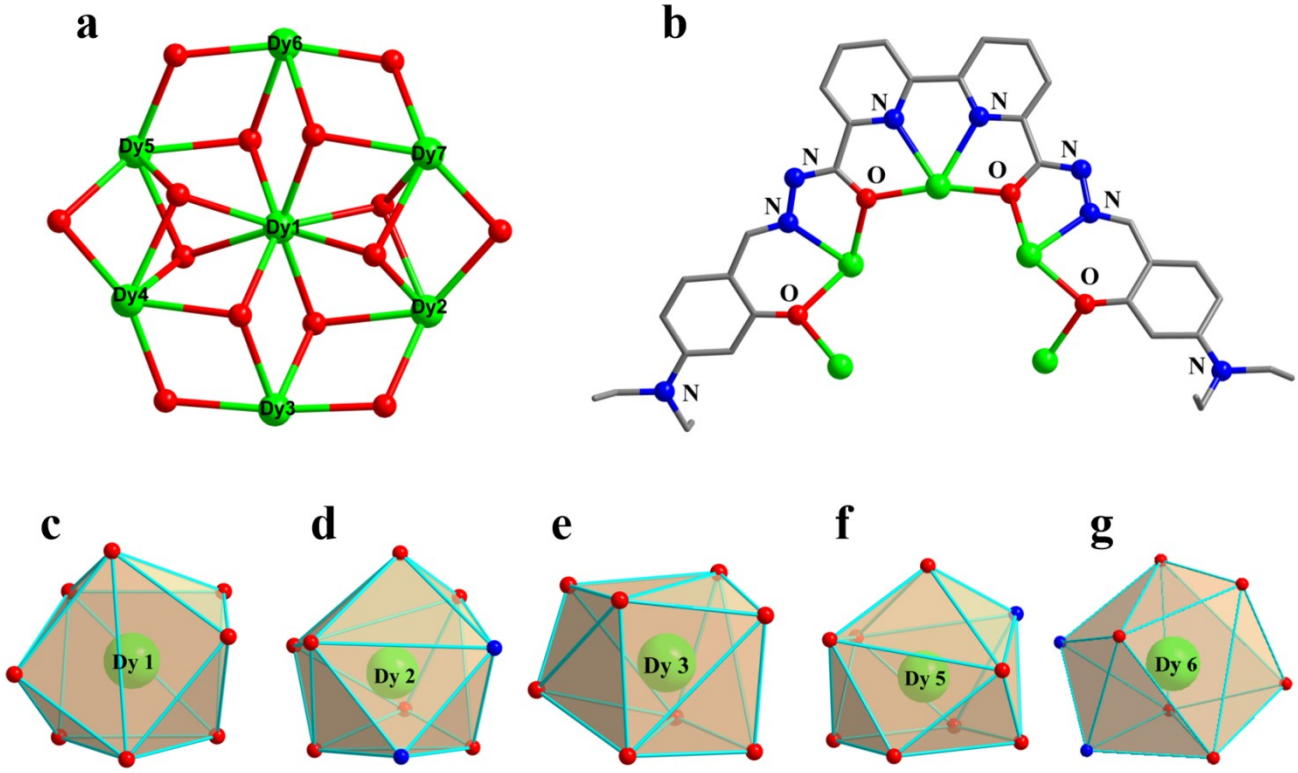

Figure S3. Cluster core of cluster **3** (a); ligand $(L^1)^{4-}$ coordination mode of cluster **3** (b); the coordination environment of metal centers Dy1, Dy2, Dy3, Dy5 and Dy6 in cluster **3** (c-g).

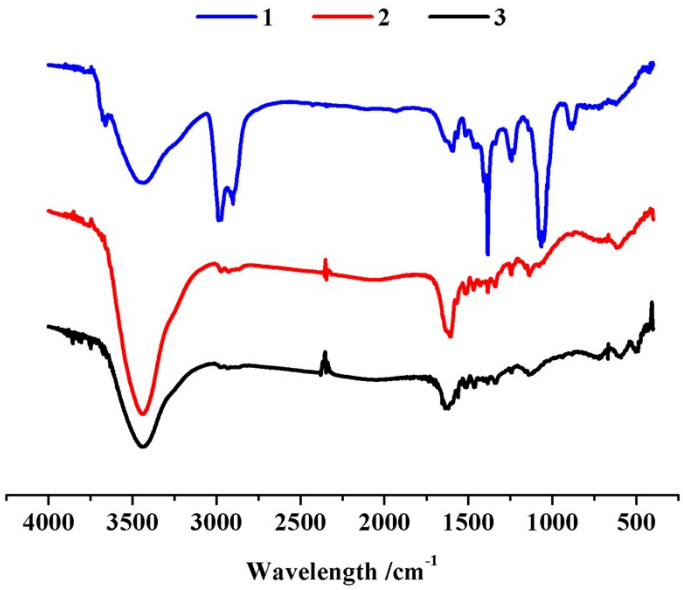

Figure S4. Infrared spectra (IR) of clusters **1**–**3**.

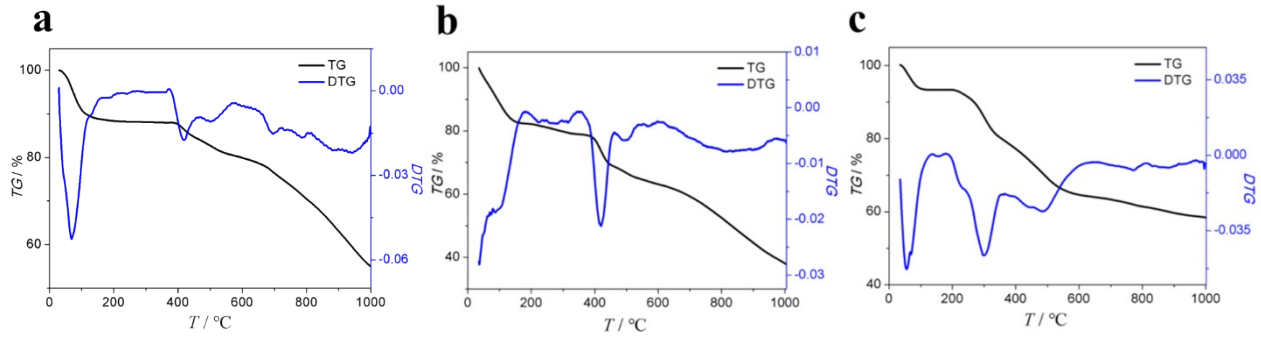

Figure S5. TG curve of clusters **1**–**3**.

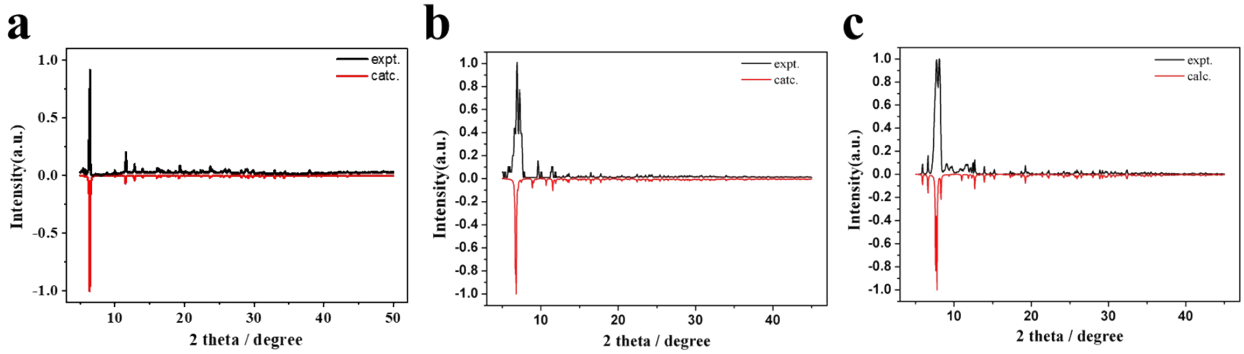

Figure S6. Powder diffraction pattern (PXRD) of clusters **1**–**3**.

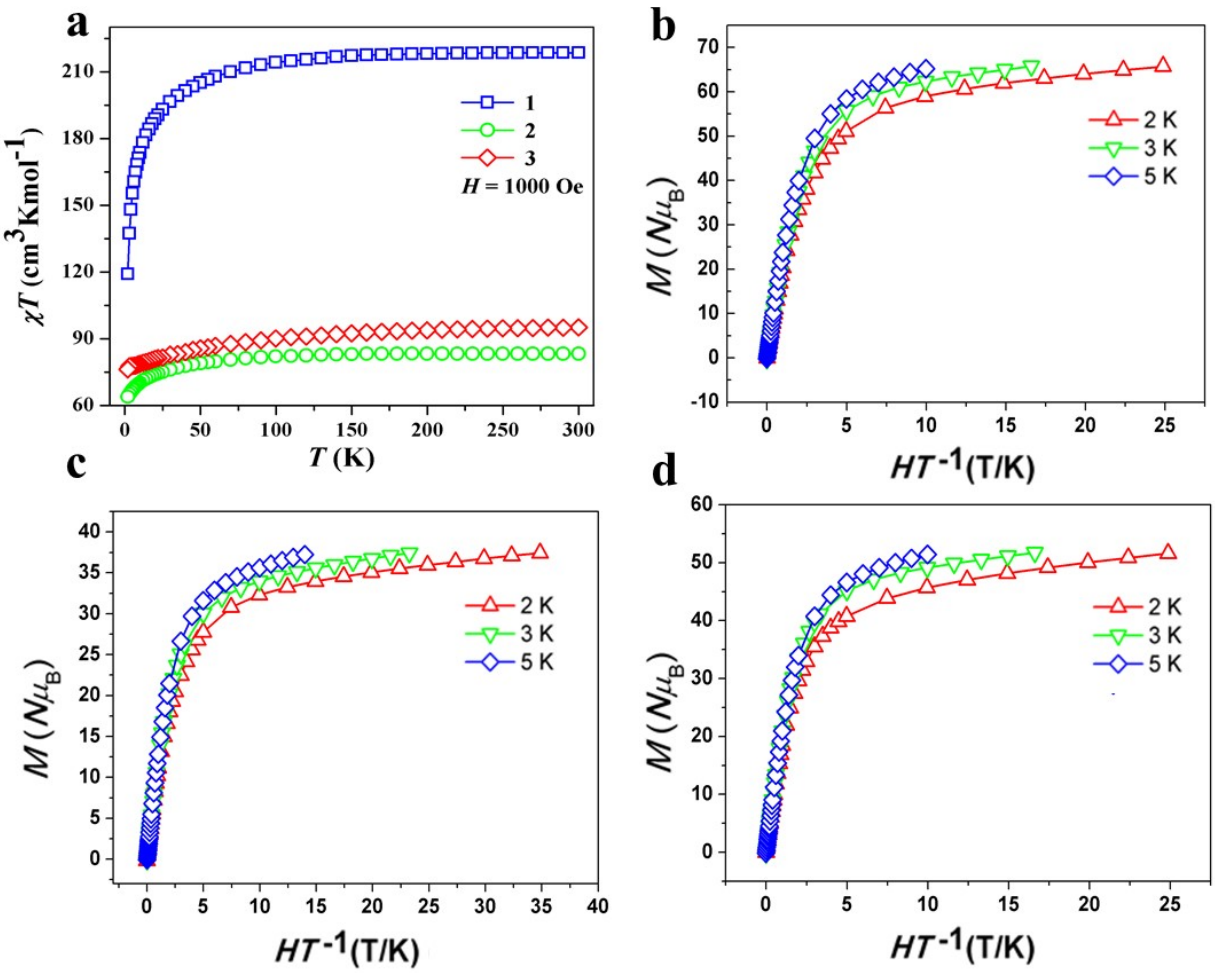

Figure S7. Temperature dependence of $\chi_m T$ for clusters **1**–**3** (a); *M* vs. *H/T* plots of clusters **1**–**3** (b, c and d).

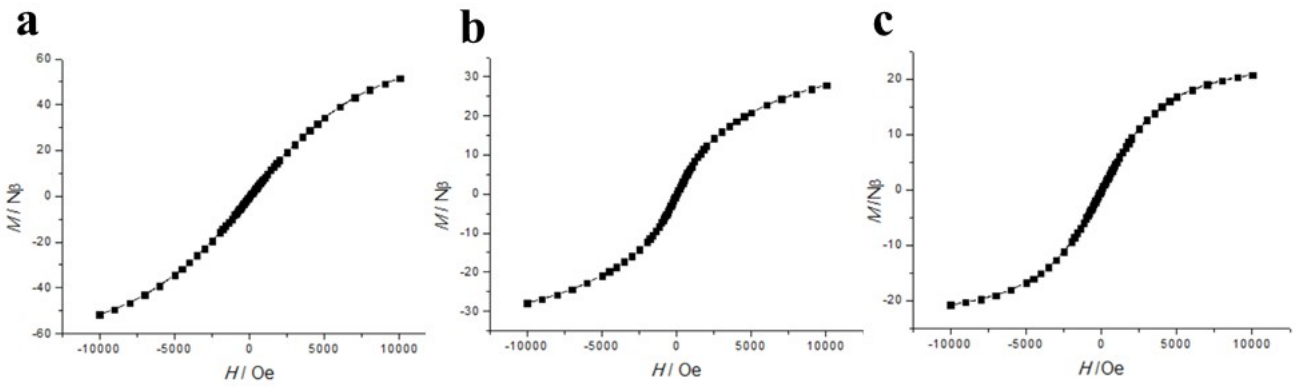

Figure 8. Loop curve graph of clusters **1**–**3** (a–c) at 2 K.

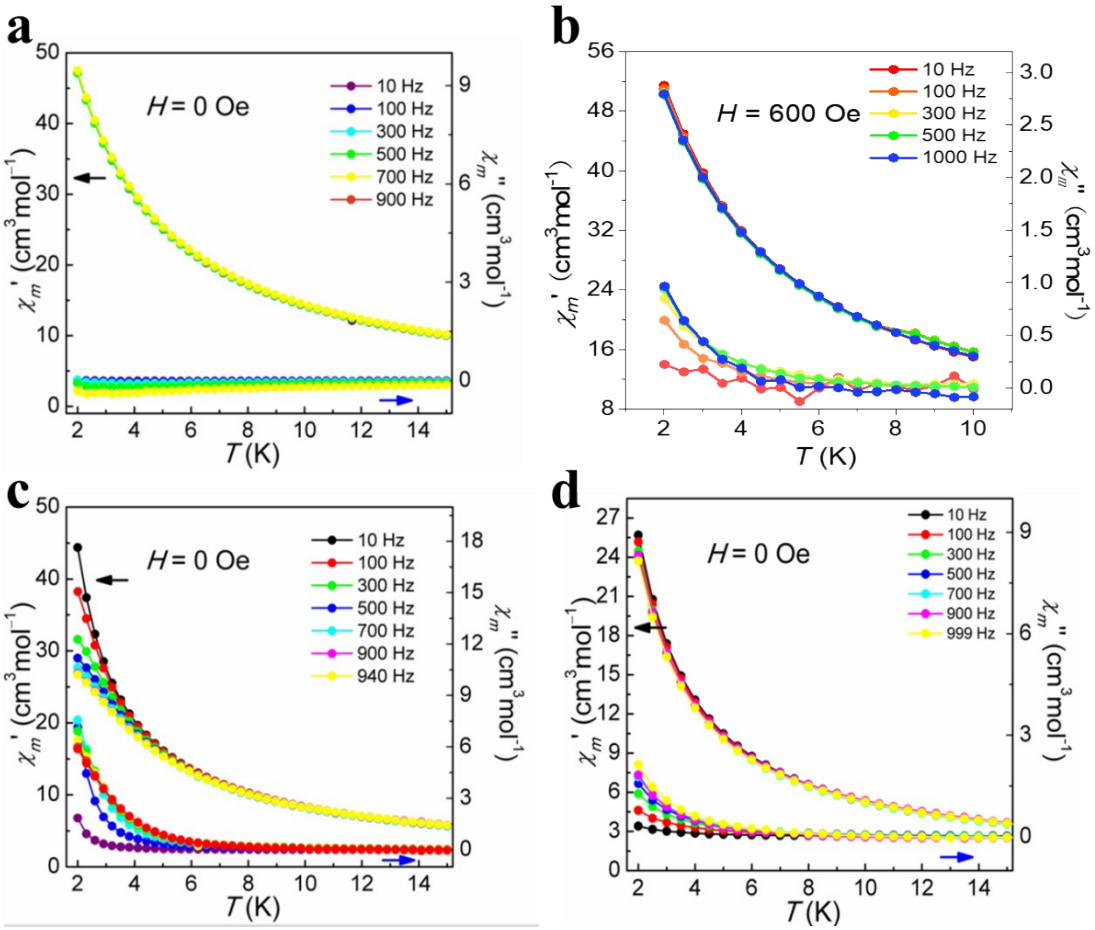

Figure S9. Temperature-dependent χ' and χ'' AC susceptibilities under 0 and 600 Oe DC fields for cluster **1** (a and b); temperature-dependent χ' and χ'' AC susceptibilities under 0 Oe DC fields for clusters **2-3** (c and d).

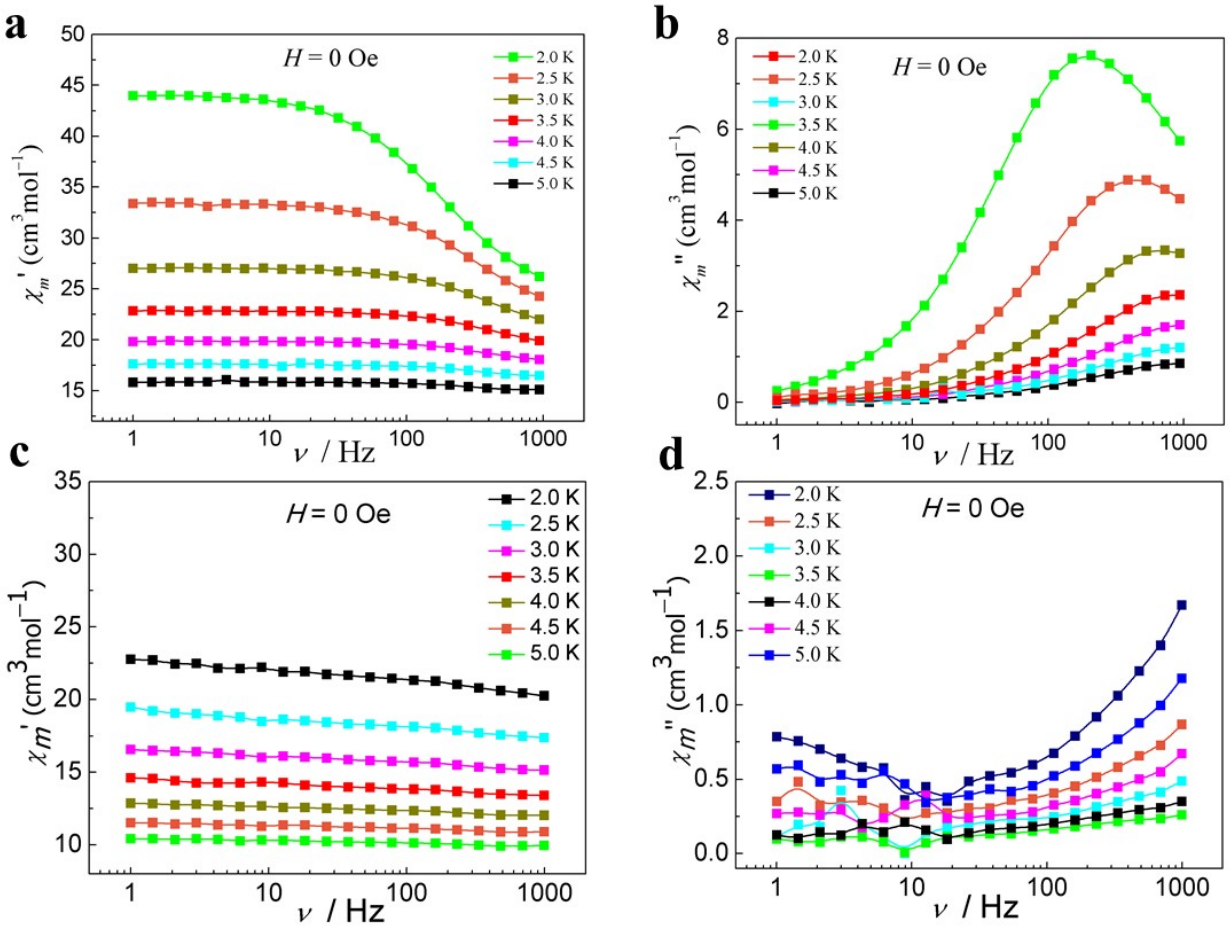

Figure S10. Frequency-dependent χ' and χ'' curves under zero fields for clusters **2** and **3**.

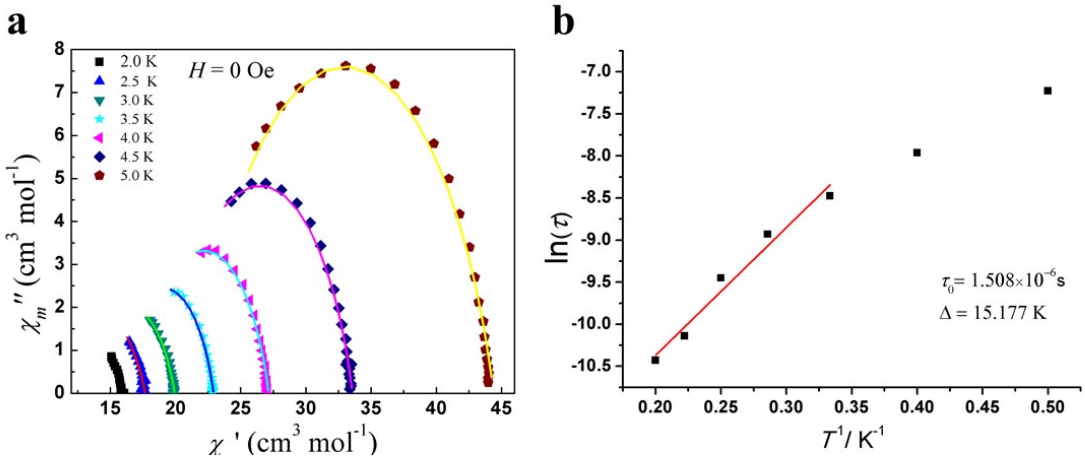

Figure S11. Cole−Cole plots for cluster **2**, solid lines are the best fits to the Debye model (a); ln(τ) vs. T^{-1} plots for cluster **2**, solid lines show the best fits with the Debye formula (linear) (b).

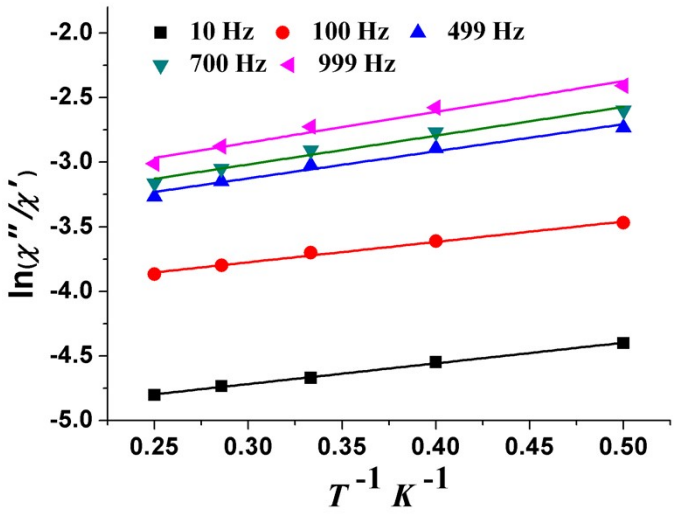

Figure S12. Plots of ln(χ''/χ') vs. T^{-1} for **3**. The solid lines represent the fitting results over the temperature range of 2–5 K.

Table S2. Selected bond lengths (Å) and angles (°) of **1**.

Bond lengths (Å)					
Dy1—O2	2.233(14)	Dy2—O1^{ii}	2.337(5)	Dy4—O7	2.423(5)
Dy1—O2^{iv}	2.233(14)	Dy2—O2^{i}	2.352(12)	Dy4—N2	2.442(7)
Dy1—O2^{iii}	2.233(14)	Dy2—O2^{iii}	2.352(11)	Dy4—O4	2.332(6)
Dy1—O6^{i}	2.336(16)	Dy2—O6^{iii}	2.284(12)	Dy4—O3^{i}	2.314(5)
Dy1—O6^{iii}	1.766(13)	Dy2—O6^{i}	2.284(12)	Dy4—O5	2.357(5)
Dy1—O6^{v}	2.336(16)	Dy3—O4	2.440(5)	Dy4—O9	2.382(6)
Dy1—O6	1.766(13)	Dy3—O4^{i}	2.440(5)	Dy4—O10	2.471(7)
Dy1—O6^{ii}	2.336(16)	Dy3—O3	2.447(5)	Dy5—O1^{ii}	2.381(5)
Dy1—O6^{iv}	1.766(13)	Dy3—O3^{i}	2.447(5)	Dy5—O1	2.381(5)
Dy1—Cl2	2.425(8)	Dy3—O5^{i}	2.380(5)	Dy5—O7	2.325(6)
Dy1—O13	2.425(8)	Dy3—O5	2.380(5)	Dy5—O7^{ii}	2.325(6)
Dy2—O3^{iii}	2.424(5)	Dy3—O2^{i}	2.412(12)	Dy5—N1	2.496(6)
Dy2—O3^{i}	2.424(5)	Dy3—O2	2.412(12)	Dy5—N1^{ii}	2.496(6)
Dy2—O5^{ii}	2.393(5)	Dy3—O6^{i}	2.403(12)	Dy5—Cl1	2.697(4)
Dy2—O5	2.393(5)	Dy3—O6	2.403(12)	Dy5—Cl1^{ii}	2.697(4)
Dy2—O1	2.337(5)	Dy4—O1	2.415(5)	Dy5—O12	2.697(4)
Bond angles (°)					

O6^{iv}—Dy1—O2^{iii}	120.9(5)	O6^{i}—Dy2—O3^{iii}	130.0(4)	O5—Dy4—N2	146.8(2)
O6^{iii}—Dy1—O6^{v}	126.1(4)	O6^{i}—Dy2—O3^{i}	78.6(4)	O1—Dy4—O7	66.24(18)
O6^{iv}—Dy1—O6^{iii}	116.1(3)	O6^{iii}—Dy2—O5^{ii}	69.2(3)	O1—Dy4—N2	129.3(2)
O6^{iii}—Dy1—O6^{ii}	58.0(7)	O6^{i}—Dy2—O5	69.3(3)	O1—Dy4—O8	67.5(3)
O6—Dy1—O6^{v}	62.4(7)	O6—Dy3—O4^{i}	137.1(3)	O1—Dy4—O10	112.9(2)
O6^{iii}—Dy1—O6	116.1(3)	O6—Dy3—O4	131.2(4)	O7—Dy4—N2	63.3(2)
O6^{ii}—Dy1—O6^{v}	79.8(5)	O6^{i}—Dy3—O4^{i}	131.2(4)	O7—Dy4—O8	119.4(3)
O6^{iv}—Dy1—O6^{v}	58.0(7)	O6^{i}—Dy3—O4	137.1(3)	O4—Dy4—O5	74.84(18)
O6^{iv}—Dy1—O6^{i}	126.1(4)	O6^{i}—Dy3—O3	120.5(3)	O4—Dy4—O9	125.5(2)
O6^{iv}—Dy1—O6	116.1(3)	O6—Dy3—O3	75.9(3)	O4—Dy4—O1	144.97(18)
O6^{iii}—Dy1—O6^{i}	62.4(7)	O6^{i}—Dy3—O3^{i}	75.9(3)	O4—Dy4—O7	125.7(2)
O6^{iv}—Dy1—O6^{ii}	62.3(7)	O6—Dy3—O3^{i}	120.5(3)	O4—Dy4—N2	74.7(2)
O6—Dy1—O6^{i}	58.0(7)	O6^{i}—Dy3—O2^{i}	19.8(3)	O4—Dy4—O8	114.6(3)
O6—Dy1—O6^{ii}	126.1(4)	O6—Dy3—O2^{i}	68.1(7)	O4—Dy4—O10	74.1(2)
O6^{ii}—Dy1—O6^{i}	79.8(5)	O6—Dy3—O6^{i}	50.5(7)	O3^{i}—Dy4—O4	75.56(19)
O6^{v}—Dy1—O6^{i}	79.8(5)	O4—Dy3—O3	95.58(18)	O3^{i}—Dy4—O5	62.48(19)
O2^{iv}—Dy1—O2	118.0(2)	O3—Dy3—O3^{i}	163.2(2)	O3^{i}—Dy4—O9	153.18(19)
O2^{iii}—Dy1—O2	118.0(2)	O5—Dy3—O4	72.47(19)	O3^{i}—Dy4—O1	76.12(18)
O6^{iii}—Dy1—O2^{iii}	19.8(5)	O5^{i}—Dy3—O4	147.49(18)	O3^{i}—Dy4—O7	77.33(18)
O6^{iii}—Dy1—O2^{iv}	120.9(5)	O5^{i}—Dy3—O4^{i}	72.47(19)	O3^{i}—Dy4—N2	97.2(2)
O6—Dy1—O2^{iv}	120.9(5)	O5—Dy3—O4^{i}	147.50(18)	O3^{i}—Dy4—O8	125.1(3)
O6^{iv}—Dy1—O2^{iv}	19.8(5)	O5^{i}—Dy3—O3	60.23(18)	O5—Dy4—O8	68.8(4)
O6—Dy1—O2^{iii}	120.9(5)	O5—Dy3—O3^{i}	60.23(18)	O5—Dy4—O10	75.9(2)
O3^{iii}—Dy2—O3^{i}	150.7(2)	O5—Dy3—O3	126.83(18)	O1—Dy5—O1^{ii}	73.1(3)
O5—Dy2—O3^{i}	60.38(18)	O5^{i}—Dy3—O3^{i}	126.83(18)	O1—Dy5—N1	123.6(2)
O5—Dy2—O3^{iii}	129.65(18)	O5^{i}—Dy3—O5	138.7(3)	O1^{ii}—Dy5—N1	143.7(2)
O5^{ii}—Dy2—O3^{iii}	60.39(18)	O5^{i}—Dy3—O2^{i}	71.7(3)	O1—Dy5—N1^{ii}	143.7 (2)
O5^{ii}—Dy2—O3^{i}	129.65(18)	O5—Dy3—O2^{i}	78.5(4)	O1^{ii}—Dy5—N1^{ii}	123.6(2)
O5—Dy2—O5^{ii}	146.9(3)	O5—Dy3—O2	71.7(3)	O1^{ii}—Dy5—Cl1	137.72 (14)
O1—Dy2—O3^{iii}	81.25(18)	O5^{i}—Dy3—O2	78.6(3)	O1^{ii}—Dy5—Cl1^{ii}	72.35(15)

O1^{ii}—Dy2—O3^{iii}	75.50(18)	O5^{i}—Dy3—O6^{i}	75.2(3)	O1—Dy5—Cl1	72.35(15)
O1^{ii}—Dy2—O3^{i}	81.26(18)	O5^{i}—Dy3—O6	67.5(3)	O1—Dy5—Cl1^{ii}	137.72(14)
O1—Dy2—O3^{i}	75.51(18)	O5—Dy3—O6^{i}	67.6(3)	O1^{ii}—Dy5—O12	137.72(14)
O1—Dy2—O5^{ii}	135.63(19)	O5—Dy3—O6	75.2(3)	O1—Dy5—O12	72.35(15)
O1^{ii}—Dy2—O5	135.63(19)	O2—Dy3—O4	113.1(4)	O7—Dy5—O1	68.33(18)
O1—Dy2—O5	74.78(19)	O2—Dy3—O4^{i}	136.3(3)	O7—Dy5—O1^{ii}	98.39(19)
O1^{ii}—Dy2—O5^{ii}	74.78(19)	O2^{i}—Dy3—O4	136.3(3)	O7^{ii}—Dy5—O1	98.39(19)
O1^{ii}—Dy2—O1	74.7(3)	O2^{i}—Dy3—O4^{i}	113.1(4)	O7^{ii}—Dy5—O1^{ii}	68.33(18)
O1—Dy2—O2^{iii}	107.1(5)	O2^{i}—Dy3—O3	128.0(3)	O7^{ii}—Dy5—O7	164.0(3)
O1—Dy2—O2^{i}	141.9(3)	O2—Dy3—O3	66.2(3)	O7—Dy5—N1	65.7(2)
O1^{ii}—Dy2—O2^{iii}	141.9(3)	O4—Dy3—O4^{i}	79.5(3)	O7^{ii}—Dy5—N1^{ii}	65.7(2)
O1^{ii}—Dy2—O2^{i}	107.1(5)	O4^{i}—Dy3—O3	71.23(18)	O7^{ii}—Dy5—N1	130.2(2)
O2^{i}—Dy2—O5	79.5(4)	O4—Dy3—O3^{i}	71.24(18)	O7—Dy5—N1^{ii}	130.2(2)
O2^{iii}—Dy2—O5	78.2(3)	O4^{i}—Dy3—O3^{i}	95.58(18)	O7^{ii}—Dy5—Cl1	93.57(17)
O6^{i}—Dy2—O5^{ii}	81.6(3)	O7—Dy4—O10	149.1(2)	O7^{ii}—Dy5—Cl1^{ii}	90.76(17)
O6^{iii}—Dy2—O5	81.6(3)	N2—Dy4—O8	137.6(3)	O7—Dy5—Cl1	90.75(17)
O6^{iii}—Dy2—O1	127.0(4)	N2—Dy4—O10	107.6(2)	O7—Dy5—Cl1^{ii}	93.58(17)
O6^{iii}—Dy2—O1^{ii}	142.7(3)	O9—Dy4—O1	88.11(19)	O7^{ii}—Dy5—O12	93.57(17)
O6^{i}—Dy2—O1^{ii}	127.0(4)	O9—Dy4—O7	76.48(19)	O7—Dy5—O12	90.75(17)
O6^{i}—Dy2—O1	142.8(3)	O9—Dy4—N2	76.0(2)	N1^{ii}—Dy5—N1	64.6(3)
O6^{i}—Dy2—O2^{iii}	75.1(7)	O9—Dy4—O8	65.1(4)	N1—Dy5—Cl1^{ii}	76.20(18)
O6^{iii}—Dy2—O2^{iii}	20.5(3)	O9—Dy4—O10	72.7(2)	N1—Dy5—Cl1	77.24(17)
O6^{i}—Dy2—O2^{i}	20.5(3)	O10—Dy4—O8	45.8(3)	N1^{ii}—Dy5—Cl1^{ii}	77.24(17)
O6^{iii}—Dy2—O2^{i}	75.1(7)	O3^{i}—Dy4—O10	133.4(2)	N1^{ii}—Dy5—Cl1	76.20(18)
O6^{iii}—Dy2—O6^{i}	57.0(8)	O5—Dy4—O9	133.9(2)	N1—Dy5—O12	77.24(17)
O6^{iii}—Dy2—O3^{i}	130.0(4)	O5—Dy4—O1	74.01(17)	N1^{ii}—Dy5—O12	76.20(18)
O6^{iii}—Dy2—O3^{iii}	78.6(4)	O5—Dy4—O7	128.80(18)		

Table S3. Selected bond lengths (Å) and angles (°) of **2**.

Bond lengths (Å)					
Dy1—O2^{i}	2.456(3)	Dy2—O2	2.322(3)	Dy2—N2	2.498(4)
Dy1—O3	2.417(3)	Dy2—O3^{i}	2.411(3)	Dy3—O1^{i}	2.371(3)
Dy1—O6	2.352(3)	Dy2—O1	2.292(3)	Dy3—O3	2.445(3)
Dy1—O9	2.329(3)	Dy2—O2^{i}	2.444(3)	Dy3—O5	2.288(4)
Dy1—N1	2.596(4)	Dy2—O2	2.322(3)	Dy3—O6	2.362(3)
Dy1—N4	2.623(4)	Dy2—O3^{i}	2.411(3)	Dy3—O7	2.218(3)
Dy1—Cl1	2.713(14)	Dy2—O4^{i}	2.343(4)	Dy3—O10	2.384(4)
Dy1—Cl2	2.687(13)	Dy2—O8	2.405(4)	Dy3—O11	2.513(4)
Dy2—O1	2.292(3)	Dy2—O9	2.372(3)	Dy3—N7	2.480(4)
Bond angles (°)					
O2^{i}—Dy1—N1	119.94(12)	N4—Dy1—Cl2	74.82(10)	O9—Dy2—N2	64.00(12)
O2^{i}—Dy1—N4	153.13(12)	Cl2—Dy1—Cl1	152.72(4)	O9—Dy2—O8	76.24(13)
O2^{i}—Dy1—Cl1	127.69(8)	N1—Dy1—Cl2	82.72(10)	O1^{i}—Dy3—O3	66.38(11)
O2^{i}—Dy1—Cl2	78.55(8)	N4—Dy1—Cl1	79.19(10)	O1^{i}—Dy3—O10	137.63(12)
O3—Dy1—O2^{i}	65.30(11)	O1—Dy2—O2^{i}	158.51(10)	O1^{i}—Dy3—O11	153.63(13)
O3—Dy1—N1	153.15(12)	O1—Dy2—O2	91.00(11)	O1^{i}—Dy3—N7	99.20(14)
O3—Dy1—N4	128.46(12)	O1—Dy2—O3^{i}	68.15(11)	O3—Dy3—O11	135.22(13)
O3—Dy1—Cl1	79.90(8)	O1—Dy2—O4^{i}	104.17(13)	O3—Dy3—N7	131.62(13)
O3—Dy1—Cl2	123.25(8)	O1—Dy2—O8	88.96(13)	O5—Dy3—O1^{i}	95.14(13)
O3—Dy1—O2^{i}	65.30(11)	O1—Dy2—O9	134.88(11)	O5—Dy3—O3	78.73(12)
O3—Dy1—N1	153.15(12)	O1—Dy2—N2	71.20(12)	O5—Dy3—O6	145.72(12)
O3—Dy1—N4	128.46(12)	O2—Dy2—O2^{i}	76.07(12)	O5—Dy3—O10	85.17(15)
O3—Dy1—Cl1	79.90(8)	O2—Dy2—O3^{i}	67.45(11)	O5—Dy3—O11	78.44(15)
O3—Dy1—Cl2	123.25(8)	O2—Dy2—O4^{i}	131.45(12)	O5—Dy3—N7	149.61(14)
O6—Dy1—O2^{i}	113.44(11)	O2—Dy2—O8	73.49(12)	O6—Dy3—O1^{i}	79.58(12)
O6—Dy1—O3	68.70(11)	O2—Dy2—O9	123.48(11)	O6—Dy3—O3	68.06(11)
O6—Dy1—N1	123.00(12)	O2^{i}—Dy2—N2	128.44(11)	O6—Dy3—O10	77.05(14)
O6—Dy1—N4	63.28(12)	O2—Dy2—N2	145.37(13)	O6—Dy3—O11	119.77(14)

O6—Dy1—Cl1	85.94(10)	O3^{i}—Dy2—O2^{i}	90.85(10)	O6—Dy3—N7	63.87(13)
O6—Dy1—Cl2	89.67(10)	O3^{i}—Dy2—N2	126.94(12)	O7—Dy3—O1^{i}	79.29(12)
O9—Dy1—O2^{i}	66.52(10)	O4^{i}—Dy2—O2^{i}	73.61(12)	O7—Dy3—O3	139.61(11)
O9—Dy1—O3	99.59(11)	O4^{i}—Dy2—O3^{i}	75.98(12)	O7—Dy3—O5	84.05(14)
O9—Dy1—O6	165.43(13)	O4^{i}—Dy2—O8	150.36(12)	O7—Dy3—O6	127.14(13)
O9—Dy1—N1	64.00(12)	O4^{i}—Dy2—O9	75.73(12)	O7—Dy3—O10	142.38(14)
O9—Dy1—N4	123.85(12)	O4^{i}—Dy2—N2	82.56(14)	O7—Dy3—O11	74.64(14)
O9—Dy1—Cl1	83.39(9)	O8—Dy2—O2^{i}	103.33(13)	O7—Dy3—N7	72.59(13)
O9—Dy1—Cl2	104.32(9)	O8—Dy2—O3^{i}	133.60(12)	O10—Dy3—O3	72.23(12)
N1—Dy1—N4	60.20(13)	O8—Dy2—N2	76.64(14)	O10—Dy3—O11	67.90(14)
N1—Dy1—Cl1	77.26(10)	O9—Dy2—O2^{i}	66.07(10)	O10—Dy3—N7	101.46(15)
O9—Dy2—O3^{i}	147.55(12)	N7—Dy3—O11	76.83(16)		

Table S4. Selected bond lengths (Å) and angles (°) of **3**.

Bond lengths (Å)					
Dy1—O1^{i}	2.407(4)	Dy2—O9	2.281(5)	Dy4—O9^{i}	2.285(5)
Dy1—O1	2.407(4)	Dy2—N11	2.661(7)	Dy4—O9	2.285(5)
Dy1—O2	2.374(5)	Dy2—N10	2.597(6)	Dy4—O11	2.397(6)
Dy1—O2^{i}	2.374 (5)	Dy3—O1	2.357(5)	Dy4—O11^{i}	2.398(7)
Dy1—O3	2.342(4)	Dy3—O2	2.404(4)	Dy4—O15^{i}	2.542(6)
Dy1—O3^{i}	2.342 (4)	Dy3—O4	2.312 (5)	Dy4—O15	2.542(6)
Dy1—O6^{i}	2.342(5)	Dy3—O5	2.361(5)	Dy5—O5^{i}	2.276(5)
Dy1—O6	2.342 (5)	Dy3—O6^{i}	2.414(5)	Dy5—O5	2.276(5)
Dy2—O1	2.474 (4)	Dy3—O10	2.505(6)	Dy5—O6	2.371(5)
Dy2—O2	2.297(5)	Dy3—N7	2.487(6)	Dy5—O6^{i}	2.371(5)
Dy2—O3^{i}	2.424(5)	Dy3—O12	2.526(7)	Dy5—N5^{i}	2.490(6)
Dy2—O4	2.348(4)	Dy3—O14	2.489(6)	Dy5—N5	2.490(6)
Dy2—O7	2.522(6)	Dy4—O3	2.331(4)	Dy5—O23^{i}	2.251(8)
Dy2—O8	2.475(6)	Dy4—O3^{i}	2.331 (4)	Dy5—O23	2.251(8)
Bond angles (°)					
O2^{i}—Dy1—O1	127.15(17)	O9—Dy2—O2	91.06(18)	O3^{i}—Dy4—O3	70.6(2)

O2—Dy1—O1	61.15(16)	O9—Dy2—O3^{i}	67.51 (16)	O3—Dy4—O11^{i}	124.1 (2)
O2^{i}—Dy1—O1^{i}	61.15(16)	O9—Dy2—O4	140.56(19)	O3—Dy4—O11	75.22(19)
O2—Dy1—O1^{i}	127.15(17)	O9—Dy2—O7	88.6(2)	O3^{i}—Dy4—O11	124.1(2)
O1—Dy1—O1^{i}	152.1(2)	O9—Dy2—O8	129.9(2)	O3^{i}—Dy4—O11^{i}	75.22(19)
O3—Dy1—O1^{i}	73.68(15)	O9—Dy2—N11	65.4(2)	O3—Dy4—O15^{i}	159.6(2)
O3^{i}—Dy1—O1^{i}	132.51(15)	O9—Dy2—N2	109.1(2)	O3^{i}—Dy4—O15^{i}	123.3(2)
O3^{i}—Dy1—O1	73.68(15)	O9—Dy2—N10	66.5(2)	O3^{i}—Dy4—O15	159.6(2)
O3—Dy1—O1	132.51(15)	N11—Dy2—N2	138.2(2)	O3—Dy4—O15	123.3(2)
O3^{i}—Dy1—O2	75.63(16)	N10—Dy2—N11	69.6(2)	O3^{i}—Dy4—N1	144.72(11)
O3—Dy1—O2	80.59(16)	N10—Dy2—N2	70.7(2)	O3—Dy4—N1	144.72 (11)
O3—Dy1—O2^{i}	75.63 (16)	O2—Dy2—N11	71.02(19)	O9^{i}—Dy4—O3^{i}	104.74(17)
O3^{i}—Dy1—O2^{i}	80.59(16)	O1—Dy3—O2	61.43(16)	O9—Dy4—O3	104.74(17)
O3—Dy1—O3^{i}	70.2(2)	O1—Dy3—O5	81.44(17)	O9^{i}—Dy4—O3	69.08(17)
O3—Dy1—O6^{i}	120.48(18)	O1—Dy3—O6^{i}	76.01(16)	O9—Dy4—O3^{i}	69.08 (17)
O3—Dy1—O6	144.55(17)	O1—Dy3—O10	155.52(19)	O9^{i}—Dy4—O9	172.8(2)
O3^{i}—Dy1—O6^{i}	144.55(16)	O1—Dy3—N7	91.24(19)	O9^{i}—Dy4—O11	102.4(2)
O3^{i}—Dy1—O6	120.48 (18)	O1—Dy3—O12	127.56(19)	O9—Dy4—O11	79.0(2)
O6^{i}—Dy1—O1	76.42(16)	O1—Dy3—O14	144.35(18)	O9—Dy4—O11^{i}	102.4(2)
O6—Dy1—O1^{i}	76.43(16)	O1—Dy3—N9	162.8(2)	O9^{i}—Dy4—O11^{i}	79.0(2)
O6^{i}—Dy1—O1^{i}	81.09(16)	O2—Dy3—O6^{i}	71.69(15)	O9—Dy4—O15^{i}	71.0(2)
O6—Dy1—O1	81.09(16)	O2—Dy3—O10	139.8(2)	O9—Dy4—O15	116.1(2)
O6^{i}—Dy1—O2	73.49(17)	O2—Dy3—N7	142.63(18)	O9^{i}—Dy4—O15	71.0(2)
O6^{i}—Dy1—O2^{i}	133.68(16)	O2—Dy3—O12	69.60(19)	O9^{i}—Dy4—O15^{i}	116.1(2)
O6—Dy1—O2	133.68(16)	O2—Dy3—O14	110.80(19)	O9^{i}—Dy4—N1	93.61(12)
O6—Dy1—O2^{i}	73.49(17)	O2—Dy3—N9	128.4(2)	O9—Dy4—N1	93.61(12)
O6—Dy1—O6^{i}	72.3(3)	O4—Dy3—O1	72.62(16)	O11—Dy4—O11^{i}	158.4(3)
O1—Dy2—O7	92.66(17)	O4—Dy3—O2	73.92(15)	O11^{i}—Dy4—O15^{i}	75.9(2)
O1—Dy2—O8	81.90(17)	O4—Dy3—O5	128.37(18)	O11—Dy4—O15^{i}	84.4(2)
O1—Dy2—N11	125.97(19)	O4—Dy3—O6^{i}	141.47 (15)	O11—Dy4—O15	75.9(2)
O1—Dy2—N2	88.50(18)	O4—Dy3—O10	119.81(18)	O11^{i}—Dy4—O15	84.4(2)

O1—Dy2—N10	155.7(2)	O4—Dy3—N7	73.72(17)	O11^{i}—Dy4—N1	79.20(15)
O2—Dy2—O1	61.17(16)	O4—Dy3—O12	111.4(2)	O11—Dy4—N1	79.20(15)
O2—Dy2—O3^{i}	75.49(16)	O4—Dy3—O14	71.88(19)	O5—Dy5—O5^{i}	165.1(2)
O2—Dy2—O4	75.28(17)	O4—Dy3—N9	95.6 (2)	O5—Dy5—O6	98.81(17)
O2—Dy2—O7	140.94(17)	O5—Dy3—O2	129.41(16)	O5—Dy5—O6^{i}	68.65(17)
O2—Dy2—O8	138.58(17)	O5—Dy3—O6^{i}	66.57(16)	O5^{i}—Dy5—O6^{i}	98.81(17)
O2—Dy2—N2	149.24(18)	O5—Dy3—O10	74.45(19)	O5^{i}—Dy5—O6	68.65(17)
O2—Dy2—N10	140.0(2)	O5—Dy3—N7	62.86(18)	O5—Dy5—N5	65.98(18)
O3^{i}—Dy2—O1	71.09(14)	O5—Dy3—O12	119.8(2)	O5—Dy5—N5^{i}	128.89(19)
O3^{i}—Dy2—O7	68.37(16)	O5—Dy3—O14	119.11(18)	O5^{i}—Dy5—N5	128.89(19)
O3^{i}—Dy2—O8	111.39(18)	O5—Dy3—N9	97.1(2)	O5^{i}—Dy5—N5^{i}	65.97(18)
O3^{i}—Dy2—N11	120.40(18)	O6^{i}—Dy3—O10	97.82(18)	O23—Dy5—O5^{i}	90.4(4)
O3^{i}—Dy2—N2	90.63(18)	O6^{i}—Dy3—N7	129.12(18)	O23—Dy5—O5	93.7(4)
O3^{i}—Dy2—N10	119.98(18)	O6^{i}—Dy3—O12	71.9(2)	O23^{i}—Dy5—O5^{i}	93.7(4)
O4—Dy2—O1	69.93(15)	O6^{i}—Dy3—O14	137.4(2)	O23^{i}—Dy5—O5	90.4(4)
O4—Dy2—O3^{i}	139.08(15)	O6^{i}—Dy3—N9	119.3(2)	O23^{i}—Dy5—O6	74.3(3)
O4—Dy2—O7	125.18(17)	O10—Dy3—O12	70.3(2)	O23—Dy5—O6^{i}	74.3(3)
O4—Dy2—O8	74.82(18)	O10—Dy3—N9	26.1(2)	O23^{i}—Dy5—O6^{i}	135.7(4)
O4—Dy2—N11	75.13 (19)	N7—Dy3—O10	74.1(2)	O23—Dy5—O6	135.7(4)
O4—Dy2—N2	100.30(18)	N7—Dy3—O12	141.1(2)	O23^{i}—Dy5—N5^{i}	81.1(4)
O4—Dy2—N10	100.79(19)	N7—Dy3—O14	75.8(2)	O23—Dy5—N5	81.1(4)
O7—Dy2—N11	141.37(19)	N7—Dy3—N9	73.1(2)	O23—Dy5—N5^{i}	72.0(3)
O7—Dy2—N2	25.47(17)	O12—Dy3—N9	68.0(3)	O23^{i}—Dy5—N5	72.0(3)
O7—Dy2—N10	74.1(2)	O14—Dy3—O10	51.58(19)	O23—Dy5—O23^{i}	148.3(5)
O8—Dy2—O7	50.95(17)	O14—Dy3—O12	70.0(2)	O6—Dy5—O6^{i}	71.3(2)
O8—Dy2—N11	126.5(2)	O14—Dy3—N9	25.5(2)	O6—Dy5—N5^{i}	126.1(2)
O8—Dy2—N2	25.57(18)	O15—Dy4—O15^{i}	49.0(3)	O6^{i}—Dy5—N5	126.1(2)
O8—Dy2—N10	73.9(2)	O15^{i}—Dy4—N1	24.49(16)	O6^{i}—Dy5—N5^{i}	142.6(2)
O9—Dy2—O1	134.78(16)	O15—Dy4—N1	24.49(16)	O6—Dy5—N5	142.6(2)

Table S5. Selected parameters from the fitting result of the Cole-Cole plots for **3** under 0 Oe fields.

Frequency (Hz)	Δ (K)	τ_0 (s)
10	1.5974	2.59×10^{-6}
100	1.5770	1.42×10^{-6}
499	2.3738	4.69×10^{-7}
700	2.0966	3.58×10^{-7}
999	2.2243	2.84×10^{-7}

Note 1

SQUEEZE results for these two compounds are as follows:

(1) Dy_{16} (1)

Loop_
_platon_squeeze_void_nr
_platon_squeeze_void_average_x
_platon_squeeze_void_average_y
_platon_squeeze_void_average_z
_platon_squeeze_void_volume
_platon_squeeze_void_count_electrons
_platon_squeeze_void_content
1 -0.111 -0.152 -0.002 8895 2808"

That is, SQUEEZE gives 2808 electrons/unit cell for the voids, and each formula unit has 2808/12 =234 electrons (since Z = 12). It is well known that 1 H_2O molecule contains 10 electrons, 1 CH_3CN molecule contains 22 electrons, and a CH_3OH molecule contains 18 electrons. Further combined with elemental analysis and thermogravimetric analysis results (Figure S5), the molecular formula of **1** is calculated to be:

$[Dy_{16}(H_4L^1)_3(Cl)_8(NO_3)_6(OH)_{24}(H_2O)_6]\cdot13CH_3OH$

(2) Dy_7 (3)

Loop_
_platon_squeeze_void_nr
_platon_squeeze_void_average_x
_platon_squeeze_void_average_y
_platon_squeeze_void_average_z
_platon_squeeze_void_volume

_platon_squeeze_void_count_electrons
_platon_squeeze_void_content

1	0.250	0.250	0.000	556	135 ' '
2	0.750	-0.250	0.000	556	135 ' '
3	0.250	-0.250	0.500	555	135 ' '
4	0.750	0.250	0.500	555	135 ' '

That is, SQUEEZE gives 135 electrons/unit cell for the voids, and each formula unit has 135/1 =135 electrons (since Z = 1). It is well known that 1 H_2O molecule contains 10 electrons, 1 CH_3CN molecule contains 22 electrons, and a CH_3OH molecule contains 18 electrons. Further combined with elemental analysis and thermogravimetric analysis results (Figure S5), the molecular formula of **3** is calculated to be:

$$[Dy_7(H_4L^1)(Cl)_2(C_{11}H_8N_2O)_2(CH_3O)_2(NO_3)_5(OH)_6(CH_3OH)_4(H_2O)_2]\cdot 10H_2O\cdot 3CH_3CN$$

References:

[1] Sheldrick, G. M. *Acta Crystallogr., Sect. C: Struct. Chem*. **2015**, *71*, 3-8.

[2] Luo, Z.-R.; Wang, H.-L.; Zhu, Z.-H.; Liu, T.; Ma, X.-F.; Wang, H.-F.; Zou, H.-H.; Liang, F.-P. Assembly of Dy_{60} and Dy_{30} Cage-Shaped Nanoclusters. *Commun. Chem.* **2020**, *3*(1), 30. https://doi.org/10.1038/s42004-020-0276-3.